Biochemistry and Biophysics Reports 17 (2019) 32–37

Contents lists available at ScienceDirect

Biochemistry and Biophysics Reports

journal homepage: www.elsevier.com/locate/bbrep

Osteoblastic differentiation improved by bezafibrate-induced mitochondrial biogenesis in deciduous tooth-derived pulp stem cells from a child with Leigh syndrome

Xu Han[a,1], Kentaro Nonaka[b,1], Hiroki Kato[a,*], Haruyoshi Yamaza[a], Hiroshi Sato[a], Takashi Kifune[a], Yuta Hirofuji[a], Keiji Masuda[a,*]

[a] Section of Oral Medicine for Children, Division of Oral Health, Growth and Development, Faculty of Dental Science, Kyushu University, 3-1-1 Maidashi, Higashi-Ku, Fukuoka 812-8582, Japan
[b] Department of Surgery and Science, Graduate School of Medical Sciences, Kyushu University, 3-1-1 Maidashi, Higashi-Ku, Fukuoka 812-8582, Japan

ARTICLE INFO

Keywords:
Bezafibrate
Dental pulp stem cell
Leigh syndrome
Mitochondrial biogenesis
Osteogenesis

ABSTRACT

Leigh syndrome is a highly heterogeneous condition caused by pathological mutations in either nuclear or mitochondrial DNA regions encoding molecules involved in mitochondrial oxidative phosphorylation, in which many organs including the brain can be affected. Among these organs, a high incidence of poor bone health has been recognized in primary mitochondrial diseases including Leigh syndrome. However, the direct association between mitochondrial dysfunction and poor bone health has not been fully elucidated. Mitochondrial biosynthesis is a potential therapeutic target for this syndrome, as it can ameliorate the impairment of oxidative phosphorylation without altering these gene mutations. A recent study has shown the impaired osteogenesis in the dental pulp stem cells derived from the deciduous teeth of a child with Leigh syndrome, harboring the heteroplasmic mutation G13513A in the mitochondrial DNA region encoding the ND5 subunit of the respiratory chain complex I. The present study aimed to investigate whether mitochondrial biogenesis could be a therapeutic target for improving osteogenesis, using the same stem cells in a patient-specific cellular model. For this purpose, bezafibrate was used because it has been reported to induce mitochondrial biogenesis as well as to improve bone metabolism and osteoporosis. Bezafibrate clearly improved the differentiation of patient-derived stem cells into osteoblasts and the mineralization of differentiated osteoblasts. The mRNA expression of peroxisome proliferator-activated receptor-gamma coactivator-1α, ATP production, and mitochondrial Ca^{2+} levels were all significantly increased by bezafibrate in the patient-derived cells. In addition, the increased amount and morphological shift from the fragmentary to network shape associated with DRP1 downregulation were also observed in the bezafibrate-treated patient-derived cells. These results suggest that mitochondrial biogenesis may be a potential therapeutic target for improving osteogenesis in patients with Leigh syndrome, and bezafibrate may be one of the candidate treatment agents.

1. Introduction

Leigh syndrome (LS) is caused by pathological mutations in nuclear DNA or mitochondrial DNA (mtDNA) regions encoding factors involved in oxidative phosphorylation (OXPHOS) [1]. Although neurological symptoms, such as psychomotor retardation, are the most prominent in LS, many other organs can also be affected [1]. Recently, a high incidence of poor bone health has been identified in primary mitochondrial disease, including LS [2,3]. However, the direct effects of mitochondrial dysfunction on poor bone health have not been fully elucidated. Genetic background responsible for LS and its clinical phenotypes is highly heterogeneous. When attributed to mtDNA mutation, individual patients or organs may vary in the ratio of mutant and normal mtDNA [4]. In addition, the association between the

Abbreviations: BZF, bezafibrate; DRP1, dynamin-related protein 1; LS, Leigh syndrome; MMP, Mitochondrial membrane potential; mtDNA, mitochondrial DNA; OXPHOS, oxidative phosphorylation; PGC-1α, peroxisome proliferator-activated receptor-gamma coactivator-1α; PPAR, peroxisome proliferator-activated receptor; RC complex I, respiratory chain complex I; SHED, Stem cells from human exfoliated deciduous teeth

* Corresponding authors.
E-mail addresses: kato@dent.kyushu-u.ac.jp (H. Kato), kemasuda@dent.kyushu-u.ac.jp (K. Masuda).
[1] These authors contributed equally to this study.

https://doi.org/10.1016/j.bbrep.2018.11.003
Received 9 July 2018; Received in revised form 9 October 2018; Accepted 12 November 2018
Available online 28 November 2018
2405-5808/ © 2018 The Authors. Published by Elsevier B.V. This is an open access article under the CC BY-NC-ND license (http://creativecommons.org/licenses/BY-NC-ND/4.0/).

nuclear background and mtDNA mutation of individual patients may affect their phenotype [5]. Thus, it is difficult to comprehensively understand the pathology and establish an effective treatment strategy for LS.

Dysfunction of mitochondrial OXPHOS is reported to be improved by mitochondrial biogenesis [6]. Members of the peroxisome proliferator-activated receptor-gamma coactivator (PGC)-1 family, master regulators of mitochondrial biogenesis, comprise PGC-1α, PGC-1β, and PGC-1-related coactivator [7]. Bezafibrate (BZF), resveratrol, and 5-aminoimidazole-4-carboxamide ribonucleoside may be potential therapeutic candidates for mitochondrial diseases that directly or indirectly target PGC-1α and improve OXPHOS by promoting mitochondrial biogenesis [6].

Stem cells from human exfoliated deciduous teeth (SHED) are mesenchymal stem cells present in the dental pulp of exfoliated deciduous teeth [8]. SHED can be noninvasively collected from children and can differentiate into neurons, osteoblasts, hepatocytes, and adipocytes [8,9]. Thus, SHED may be used as a disease-specific or patient-specific cellular model to elucidate the pathology and identify therapeutic targets of diseases. A recent study demonstrated the impaired osteogenesis in SHED derived from a child with LS, harboring the G13513A mutation in the mtDNA region encoding the ND5 subunit of respiratory chain (RC) complex I [10].

This study aimed to investigate the effect of mitochondrial biogenesis on osteogenesis in this patient. For this purpose, BZF, a pan peroxisome proliferator-activated receptor (PPAR) agonist, was used as a mitochondrial biogenesis inducer because BZF also has regulatory effects on bone metabolism and osteoporosis [11,12]. The effect of BZF on mitochondrial biogenesis and osteogenesis was examined using SHED derived from this patient as a cellular model.

2. Materials and methods

2.1. Isolation and culture of SHED

Experiments using human samples were reviewed and approved by the Kyushu University Institutional Review Board for Human Genome/Gene Research (permission number: 678-00) and were conducted in accordance with the Declaration of Helsinki. Informed consent was obtained from the patient's guardians. Deciduous teeth were collected from a healthy control and a child with LS at 4 and 6 years of age, respectively. SHED were isolated from dental pulp tissues as described previously [10], and grown in a SHED culture medium consisting of Minimum Essential Medium Eagle Alpha Modification (Sigma-Aldrich, MO, USA) with 15% fetal bovine serum (Sigma-Aldrich), 100 μM L-ascorbic 2-phosphate (Wako Pure Chemical Industries, Osaka, Japan), 2 mM L-glutamine (Life Technologies, NY, USA), 100 U/mL penicillin (Life Technologies), 100 μg/mL streptomycin (Life Technologies) and 25 μg/mL Fungizone (Life Technologies) at 37 °C in 5% CO_2. SHED were used at passage 4–6.

2.2. Osteogenic differentiation of SHED

The cells ($4.5 \times 10^4/cm^2$) were cultured in 6-well plates to confluence. For osteoblast differentiation, the cells were cultured in differentiation medium composed of the culture medium described above, supplemented with 1.8 mM potassium dihydrogen phosphate (Nacalai Tesque, Kyoto, Japan) and 10 nM dexamethasone (Sigma-Aldrich). LS cells were differentiated in the presence or absence of 100 μM BZF (Sigma-Aldrich). The cells were differentiated for 4 weeks for examination by Alizarin Red-S staining, and for 1 week for other experiments. The medium was changed twice a week.

2.3. Quantitative reverse transcription polymerase chain reaction (RT-qPCR)

Total RNA extraction and RT-qPCR were performed as described previously [10]. The sequences of the primer sets used in this study were as follows: alkaline phosphatase (ALP), 5′-ACGTGGCTAAGAATG TCATC-3′ (ALP forward) and 5′-CTGGTAGGCGATGTCCTTA-3′ (ALP reverse); and PGC-1α, 5′- GGCAGAAGGCAATTGAAGAG-3′ (PGC-1α forward) and 5′-TCAAAACGGTCCCTCAGTTC-3′ (PGC-1α reverse); and 18S rRNA, 5′-CGGCTACCACATCCAAGGAA-3′ (18S rRNA forward) and 5′-GCTGGAATTACCGCGGCT-3′ (18S rRNA reverse). The relative expression levels of the target genes were analyzed using the comparative threshold cycle method by normalizing to them to the levels of 18S rRNA.

2.4. Alizarin Red-S staining

SHED were fixed with 4% paraformaldehyde (Wako Pure Chemical Industries) in 0.1 M sodium phosphate buffer (pH 7.4) for 10 min at room temperature and washed thrice with phosphate-buffered saline. The cells were then rinsed with dH_2O and stained with 1% Alizarin Red-S (pH 4.2; Sigma-Aldrich) for 30 s. To quantify Alizarin Red-S staining, 10% (v/w) cetylpyridinium chloride (Nacalai Tesque) in 10 mM sodium phosphate buffer (pH 7.0) was used to extract Alizarin Red-S, the absorbance of which was measured at 570 nm using an Infinite 200 PRO plate reader (Tecan, Männedorf, Switzerland).

2.5. Measurement of mitochondrial calcium levels

To measure mitochondrial calcium, the cells were cultured in 96-well plates and stained with 10 μM Rhod-2 AM (Life Technologies) and 0.05% (w/v) Pluronic F-127 in HBSS for 45 min at 37 °C. The fluorescence signals were measured by excitation at 552 nm and emission at 581 nm, using an Infinite 200 PRO plate reader (Tecan).

2.6. Measurement of mitochondrial membrane potential

Mitochondrial membrane potential (MMP) was measured by staining with JC-1 (Life Technologies) as described previously [10]. Populations of 10,000 cells were analyzed for each sample, and green and red JC-1 signals were detected using the FL1 and FL2 channels of a FACSCalibur (BD Bioscience, CA, USA) flow cytometer, respectively. The geometric means of FL1 and FL2 were measured using CellQuest software (BD Bioscience), and the FL2/FL1 ratio was calculated.

2.7. Measurement of intracellular ATP levels

The cells were harvested in ice-cold PBS. To measure intracellular ATP levels, CellTiter-Glo Luminescent Cell Viability Assay (Promega, WI, USA) was used to measure intracellular ATP levels. The ATP levels were normalized to the protein content of the samples.

2.8. Immunocytochemistry

Cells cultured on coverslips were fixed with 4% paraformaldehyde in 0.1 M sodium phosphate buffer (pH 7.4) for 10 min at room temperature and then permeabilized with 0.1% Triton X-100 in PBS for 5 min. The cells were blocked with 2% bovine serum albumin (BSA; Wako Pure Chemical Industries) in PBS for 20 min and then incubated with anti-Tom20 antibody (1:200, #sc-11415, Santa Cruz Biotechnology, CA, USA). After 90 min, the cells were incubated with Alexa Fluor-conjugated secondary antibodies (Life Technologies) in the

dark for 60 min. After staining with antibodies, the nuclei were stained with 1 μg/mL of 4′,6-diamidino-2-phenylindole dihydrochloride (DAPI; Dojindo, Kumamoto, Japan). The cells were then mounted using ProLong Diamond (Life Technologies). The fluorescence images were captured using an Axio Imager M2 (Zeiss, Oberkochen, Germany) equipped with ApoTome2 (Zeiss). To examine the amount of mitochondria, five fluorescence images of each cell were captured. The Tom20-stained area of each image was measured using Fiji software [13] and divided by the number of nuclei.

2.9. Western blot analysis

Total cellular protein (6 μg per lane) was fractionated by 10% SDS-PAGE and transferred to PVDF membranes (Millipore, CA, USA). Membranes were incubated with antibodies against active β-catenin (1:1000, #8814S, Cell Signaling Technology, MA, USA), dynamin-related protein 1 (1:2000, DRP1; #611113, BD Biosciences, Franklin Lakes, NJ, USA) and α-Tubulin (1:2000, #sc-32293, Santa Cruz Biotechnology). Protein bands were visualized using ECL Prime Western Blotting Detection Reagent (GE Healthcare, Little Chalfont, UK), and analyzed using a LAS 1000 pro (GE Healthcare). The ratio of the signals for DRP1/α-tubulin was used to estimate the relative protein levels.

2.10. Statistical analysis

Statistical analyses were performed by Student's *t*-test using JMP software version 12 (SAS Institute, NC, USA). P values < 0.05 were considered to indicate statistically significant differences.

3. Results

3.1. Positive effect of BZF on in vitro osteogenesis in LS cells

As reported previously, the intensity of Alizarin red staining in osteoblasts differentiated from SHED derived from the patient (LS-OB) was significantly lower than that of osteoblasts differentiated from SHED derived from the healthy control (Ctrl-OB) [10]. However, the intensity of Alizarin red staining of LS-OB supplemented with BZF was significantly increased compared to that of LS-OB without BZF (Fig. 1 A). Consistently, osteogenic differentiation markers, mRNA expression of ALP and protein expression of active β-catenin, were increased in LS-OB supplemented with BZF to levels similar to that in Ctrl-OB (Fig. 1 B, C). These data suggested that BZF has a positive effect on the impaired osteogenesis of LS-OB.

3.2. Intracellular ATP production, mitochondrial Ca^{2+} levels, and MMP affected by BZF in LS cells

The mitochondrial function of LS-OB supplemented with BZF was examined. Both the intracellular ATP levels and the mitochondrial Ca^{2+} levels were increased in the LS-OB supplemented with BZF to a level similar to that in Ctrl-OB (Fig. 2 A and B). However, BZF had no effect on MMP (Fig. 2 C). These data indicated that BZF restores the mitochondrial function of LS-OB without alteration of MMP.

3.3. PGC-1α expression, mitochondrial biogenesis, and morphology affected by BZF in LS cells

In LS-OB, mRNA expression of PGC-1α, a master regulator of mitochondrial biogenesis, was significantly lower than that in Ctrl-OB, and BZF restored it to a level similar to that in Ctrl-OB (Fig. 3 A). Regarding mitochondrial morphology, fragmented mitochondria significantly increased in LS-OB compared to those in Ctrl-OB (Fig. 3 B, C). In LS-OB supplemented with BZF, while fragmented mitochondria were reduced, an elongated mitochondrial network similar to that in Ctrl-OB was observed (Fig. 3 B, C). Quantitative analysis showed a lower amount of mitochondria per cell of LS-OB compared to that of Ctrl-OB, which was restored by BZF to levels comparable to that in Ctrl-OB (Fig. 3 D). In addition, increased expression of DRP1, a master molecule of mitochondrial fission, was observed in LS-OB, which was significantly reduced by BZF (Fig. 3 E). These data suggest that mitochondrial biogenesis, associated with mitochondrial network formation by downregulation of DRP1, was promoted through the BZF-PGC-1α pathway in LS-OB.

4. Discussion

In the present study, BZF effectively restored the attenuated osteogenesis of SHED derived from a child with LS, harboring the G13513A mutation in the mtDNA. Furthermore, the expression of PGC-1α, ATP production, and mitochondrial Ca^{2+} levels were all elevated by BZF, which was associated with enhanced mitochondrial biogenesis and network formation.

Although patient-derived stem cells will be promising cellular models for investigating the underlying pathology and therapeutic strategy of mitochondrial defects, the heteroplasmic state should be considered to translate *in vitro* analysis to patients with mtDNA mutations [14–16]. In our patient, the ratio of G13513A mutant mtDNA was at least 50% in the peripheral blood. This ratio was maintained during the culture of SHED derived from this patient (Suppl. Fig. A). In addition, SHED was directly differentiated into osteoblasts, which minimized the potential risk factors of introducing new mtDNA mutations, such as those associated with reprogramming [17]. The cellular model tested in this study might thus reflect the *in vivo* mitochondrial dysfunction in this patient.

To test the effect of BZF on osteogenesis using SHED with these features, 100 μM BZF was supplemented to the medium. This concentration has been shown to promote *in vitro* osteogenic differentiation of MC3T3-E1 cell line [18]. Because BZF has not yet been clinically applied as a therapeutic agent for mitochondrial disease, the optimum concentration remains unknown. However, during the *in vitro* osteogenic induction of LS-SHED, BZF showed positive effects on mitochondrial activation and biogenesis, associated with the induction of PGC-1α expression. PPARs, the target of BZF, include three subtypes, α, δ/β, and γ, which may be expressed under tissue-specific regulation [19]. Although the PPAR subtypes were not analyzed in this study, all subtypes can induce PGC-1α expression via the peroxisome proliferator response element at the promoter region of the PGC-1α gene [20–22]. In this model, BZF may promote PGC-1α-mediated mitochondrial biogenesis by activating any of the PPAR subtypes. However, the MMP was not improved by BZF, suggesting that BZF has no effect on the intrinsic defect of RC complex I in this model. Increased mitochondrial ATP production and Ca^{2+} levels, both of which require MMP, in BZF-treated LS-OB might be due to the quantitative increase in expression of RC complexes and calcium transporters associated with mitochondrial biogenesis via the BZF-PPAR-PGC-1α pathway.

The metabolic shift from glycolysis to OXPHOS during stem cell differentiation requires mitochondrial biogenesis as well as mitochondrial elongation and network formation [23]. Mitochondrial fragmentation has been observed in fibroblasts derived from patients with respiratory chain complex I deficiency [24]. The morphological shift from fragmentary to network shape observed in this study suggests the BZF-mediated association between mitochondrial biogenesis and

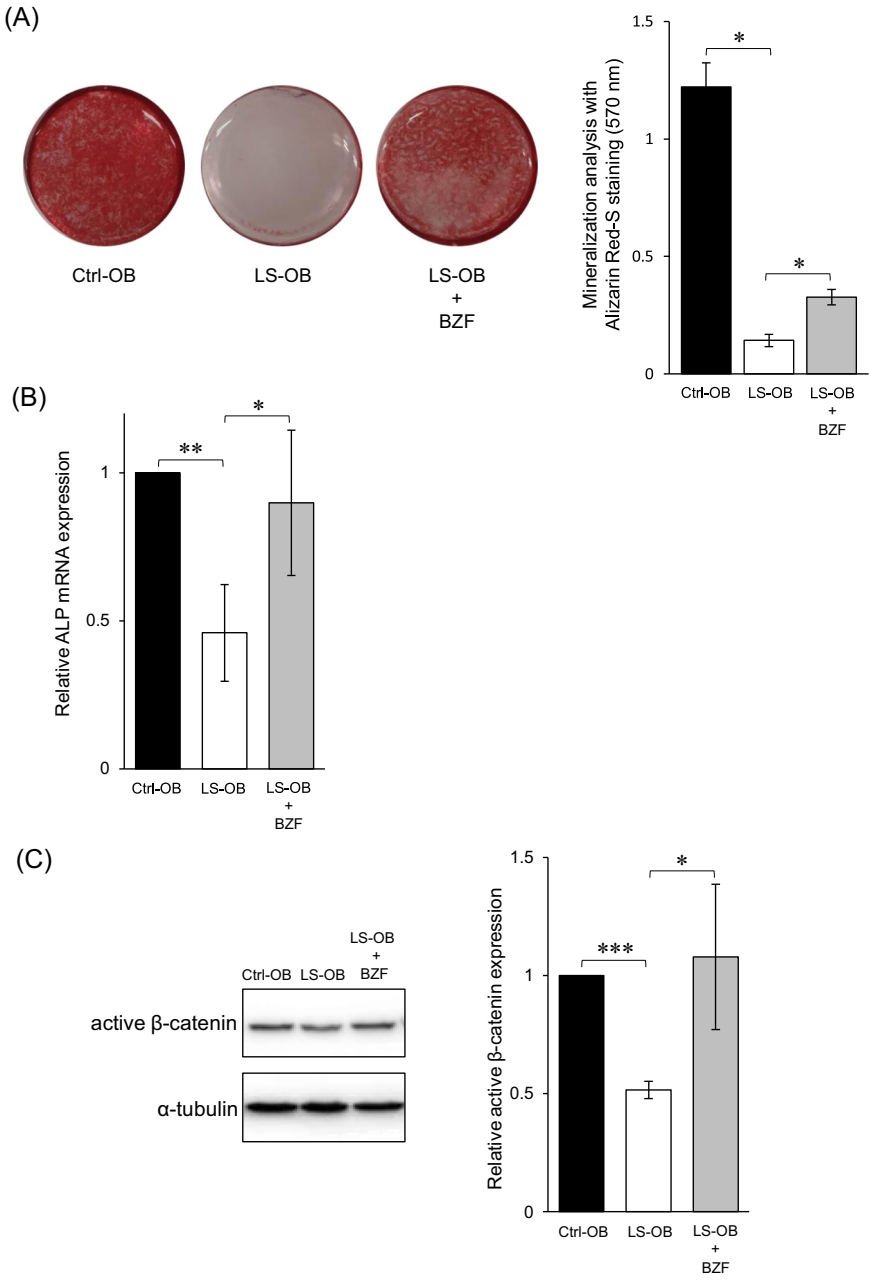

Fig. 1. Positive effect of bezafibrate (BZF) on osteogenesis of LS cells. (A) OBs were stained with Alizarin Red-S, which was extracted and measured by absorbance at 570 nm. Data represent the mean ± standard deviation from three experiments. *P < 0.05. (B) The expression of ALP mRNA in OBs was measured by RT-qPCR. The relative difference was calculated, and the level of Ctrl-OB was set as 1. Data represent the mean ± standard deviation from three experiments. *P < 0.05, **P < 0.01. (C) The protein expression of active β-catenin was measured by western blotting. The relative difference was calculated, and the level of Ctrl-OB was set as 1. Data represent the mean ± standard deviation from three experiments. *P < 0.05, ***P < 0.001.

morphology. PGC-1α has been shown to regulate several molecules involved in mitochondrial fusion and fission, including DRP1 [25]. In addition, inhibition of the mitochondrial fission by DRP1 deficiency was essential to induce mitochondrial fusion in neurons [26]. Although mitochondrial morphology is regulated by many molecules, the downregulation of DRP1 might be one of the effects of the BZF-PGC-1α pathway in accelerating mitochondrial fusion and network formation.

There are several limitations in this study, considering the genotype-phenotype correlation and therapeutic targets of LS. First, *in vivo* administration of BZF in mouse models with mitochondrial defects has shown variable outcomes, depending on their genetic backgrounds, target organs and dose of BZF [27]. Second, the main organs affected in LS are the brain, heart, liver, and kidney [1]. BZF might not always be effective for all symptoms of LS, as the ratio of heteroplasmy and factors involved in mitochondrial biogenesis may vary with organs in a patient. Third, *in vivo* bone formation and metabolism are regulated by osteoblasts as well as osteoclasts [28–30]. It is impossible to conclude that the effect of BZF on osteoblasts is sufficient to improve osteogenesis in LS. Many experiments are necessary to resolve these questions, including *in vivo* administration of BZF to mouse models of LS, and the establishment of experimental systems to examine drugs by differentiation of SHED derived from patients to other cell lineages such as neurons, muscles, and osteoclasts.

In conclusion, the present study, by using SHED derived from a child with LS characterized by the G13513A mutation in mtDNA, demonstrated that PGC-1α-mediated mitochondrial biogenesis may be a therapeutic target for improving osteogenesis in LS and that BZF may be one of the potential candidates (Suppl. Fig. B).

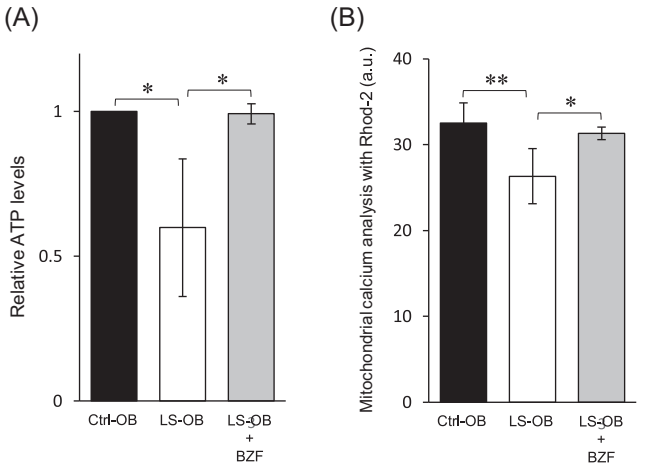

Fig. 2. Effect of bezafibrate (BZF) on mitochondrial function of LS cells. (A) The intracellular ATP levels in OBs were measured using an ATP luminescence assay. The relative difference was calculated, and the level of Ctrl-OB was set as 1. Data represent the mean ± standard deviation from three experiments. *P < 0.05. (B) Mitochondrial calcium levels were measured by Rhod-2 AM staining. The fluorescence intensity of Rhod-2 AM is shown in the graph. Data represent the mean ± standard deviation from three experiments. *P < 0.05, **P < 0.01. a.u., arbitrary unit. (C) MMP was measured by JC-1 staining. JC-1 red and green fluorescence signals were analyzed by flow cytometry. The relative differences in the ratio of red/green fluorescence were calculated, and the ratio of red/green fluorescence in Ctrl-OB was set as 1. Data represent the mean ± standard deviation from three experiments. *P < 0.05; n.s., not significant.

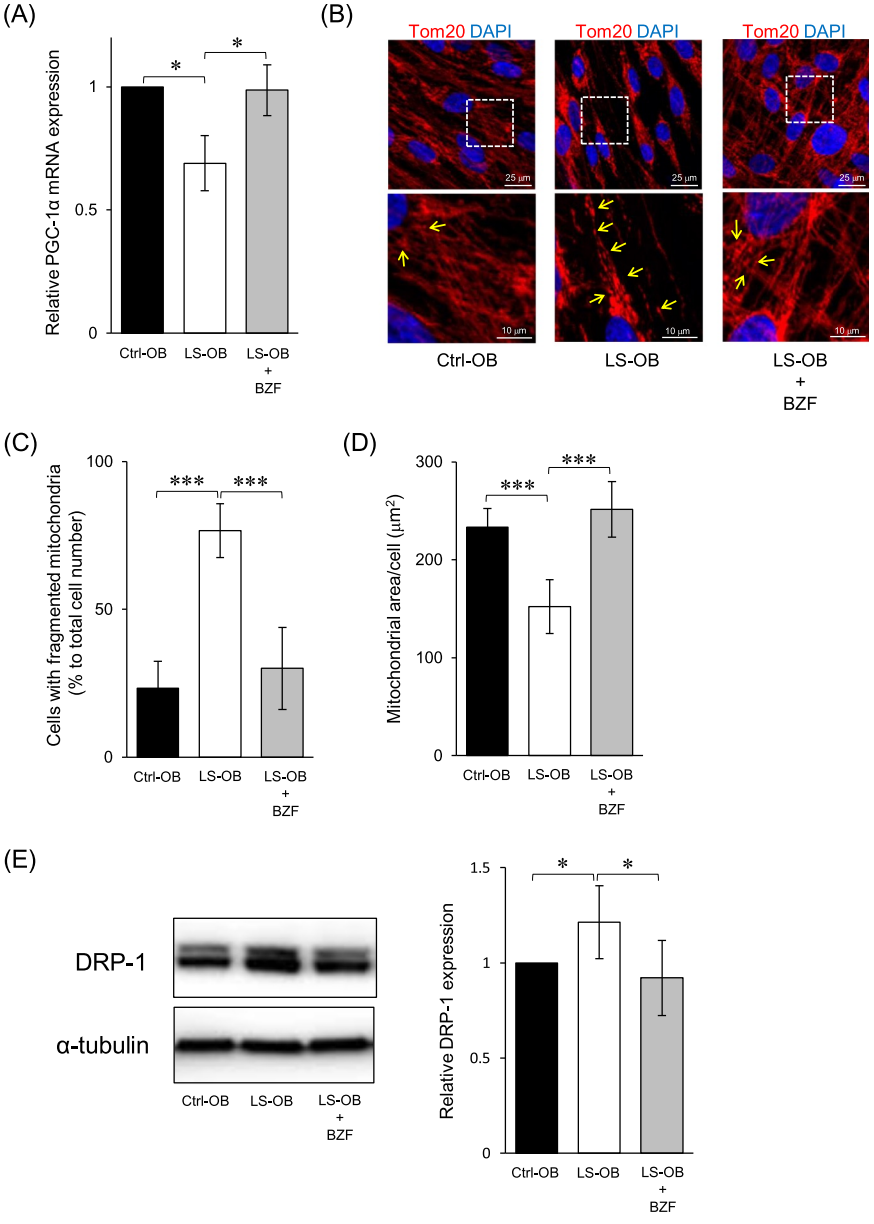

Fig. 3. Effect of bezafibrate (BZF) in mitochondrial biogenesis and morphology of LS cells. (A) The expression of PGC-1α in OBs was measured by RT-qPCR. The relative difference was calculated, and the level of Ctrl-OB was set as 1. Data represent the mean ± standard deviation from three experiments. *P < 0.05. (B) The cells were immunostained with anti-Tom20 antibody (a mitochondrial marker), and counterstained with DAPI. Details of the boxed region in the upper panels are shown in the lower panels. Yellow arrows indicate fragmented mitochondria. (C) The number of cells with fragmented mitochondria was counted. The percentage to total cell number was calculated. Data represent the mean ± standard deviation from the analysis of thirty cells from five immunostained images. ***P < 0.001. (D) The fluorescence intensity of Tom20 in the stained area was measured and divided by the number of nuclei for quantitative analysis. Data represent the mean ± standard deviation from the analysis of four immunostained images. ***P < 0.001. (E) DRP1 expression in OBs was analyzed by immunoblotting. DRP1 expression was normalized to α-Tubulin expression. DRP1 expression in Ctrl-OB was set as 1. The mean ± SEM from three experiments is shown. *P < 0.05.

Acknowledgments

We thank all the members of the Department of Pediatric Dentistry and Special Needs Dentistry at Kyushu University Hospital for their valuable suggestions, technical support, and materials. We appreciate the technical assistance provided by the Research Support Center at the Research Center for Human Disease Modeling, Kyushu University Graduate School of Medical Sciences.

Funding

This work was supported by the Takeda Science Foundation and the Kaibara Morikazu Medical Science Promotion Foundation, Japan.

Appendix A. Transparency document

Supplementary data associated with this article can be found in the online version at doi:10.1016/j.bbrep.2018.11.003.

Appendix B. Supplementary material

Supplementary data associated with this article can be found in the online version at doi:10.1016/j.bbrep.2018.11.003.

References

[1] J. Finsterer, Leigh and Leigh-like syndrome in children and adults, Pediatr. Neurol. 39 (2008) 223–235.
[2] S. Parikh, A. Goldstein, A. Karaa, M.K. Koenig, I. Anselm, C. Brunel-Guitton, J. Christodoulou, B.H. Cohen, D. Dimmock, G.M. Enns, M.J. Falk, A. Feigenbaum, R.E. Frye, J. Ganesh, D. Griesemer, R. Haas, R. Horvath, M. Korson, M.C. Kruer, M. Mancuso, S. McCormack, M.J. Raboisson, T. Reimschisel, R. Salvarinova, R.P. Saneto, F. Scaglia, J. Shoffner, P.W. Stacpoole, C.M. Sue, M. Tarnopolsky, C. Van Karnebeek, L.A. Wolfe, Z.Z. Cunningham, S. Rahman, P.F. Chinnery, Patient care standards for primary mitochondrial disease: a consensus statement from the Mitochondrial Medicine Society, Genet. Med. (2017), https://doi.org/10.1038/gim.2017.107.
[3] S.S. Gandhi, C. Muraresku, E.M. McCormick, M.J. Falk, S.E. McCormack, Risk factors for poor bone health in primary mitochondrial disease, J. Inherit. Metab. Dis. (2017) 1–11, https://doi.org/10.1007/s10545-017-0046-2.
[4] A. Fayssoil, P. Laforêt, W. Bougouin, C. Jardel, A. Lombès, H.M. Bécane, N. Berber, T. Stojkovic, A. Béhin, B. Eymard, D. Duboc, K. Wahbi, Prediction of long-term prognosis by heteroplasmy levels of the m.3243A > G mutation in patients with the mitochondrial encephalomyopathy, lactic acidosis and stroke-like episodes syndrome, Eur. J. Neurol. 24 (2017) 255–261.
[5] P. Bénit, R. El-Khoury, M. Schiff, A. Sainsard-Chanet, P. Rustin, Genetic background influences mitochondrial function: modeling mitochondrial disease for therapeutic development, Trends Mol. Med. 16 (2010) 210–217.
[6] T. Valero, Mitochondrial biogenesis: pharmacological approaches, Curr. Pharm. Des. 20 (2014) 5507–5509.
[7] R.C. Scarpulla, Metabolic control of mitochondrial biogenesis through the PGC-1 family regulatory network, Biochim. Biophys. Acta 2011 (1813) 1269–1278.
[8] M. Miura, S. Gronthos, M. Zhao, B. Lu, L.W. Fisher, P.G. Robey, S. Shi, SHED: stem cells from human exfoliated deciduous teeth, Proc. Natl. Acad. Sci. USA 100 (2003) 5807–5812.
[9] N. Ishkitiev, K. Yaegaki, B. Calenic, T. Nakahara, H. Ishikawa, V. Mitiev, M. Haapasalo, Deciduous and permanent dental pulp mesenchymal cells acquire hepatic morphologic and functional features in vitro, J. Endod. 36 (2010) 469–474.
[10] H. Kato H, X. Han, H. Yamaza, K. Masuda, Y. Hirofuji, H. Sato, T.T.M. Pham, T. Taguchi, K. Nonaka, Direct effects of mitochondrial dysfunction on poor bone health in Leigh syndrome, Biochem. Biophys. Res. Commun. 493 (2017) 207–212.
[11] K. Still, P. Grabowski, I. Mackie, M. Perry, N. Bishop, The peroxisome proliferator activator receptor alpha/delta agonists linoleic acid and bezafibrate upregulate osteoblast differentiation and induce periosteal bone formation in vivo, Calcif. Tissue Int. 83 (2008) 285–292.
[12] A. Tenenbaum, E.Z. Fisman, Balanced pan-PPAR activator bezafibrate in combination with statin: comprehensive lipids control and diabetes prevention? Cardiovasc. Diabetol. 11 (2012) 140.
[13] J. Schindelin, I. Arganda-Carreras, E. Frise, V. Kaynig, M. Longair, T. Pietzsch, S. Preibisch, C. Rueden, S. Saalfeld, B. Schmid, J.Y. Tinevez, D.J. White, V. Hartenstein, K. Eliceiri, P. Tomancak, A. Cardona, Fiji: an open-source platform for biological-image analysis, Nat. Methods 9 (2012) 676–682.
[14] A. Prigione, Induced pluripotent stem cells (iPSCs) for modeling mitochondrial DNA disorders, Methods Mol. Biol. 1265 (2015) 349–356.
[15] H. Hatakeyama, Y. Goto, Concise review: heteroplasmic mitochondrial DNA mutations and mitochondrial diseases: toward iPSC-based disease modeling, drug discovery, and regenerative therapeutics, Stem Cells 34 (2016) 801–808.
[16] G. Inak, C. Lorenz, P. Lisowski, A. Zink, B. Mlody, A. Prigione, Concise review: induced pluripotent stem cell-based drug discovery for mitochondrial disease, Stem Cells 35 (2017) 1655–1662.
[17] A. Prigione, B. Lichtner, H. Kuhl, E.A. Struys, M. Wamelink, H. Lehrach, M. Ralser, B. Timmermann, J. Adjaye, Human induced pluripotent stem cells harbor homoplasmic and heteroplasmic mitochondrial DNA mutations while maintaining human embryonic stem cell-like metabolic reprogramming, Stem Cells 29 (2011) 1338–1348.
[18] X. Zhong, L.L. Xiu, G.H. Wei, Y.Y. Liu, L. Su, X.P. Cao, Y.B. Li, H.P. Xiao, Bezafibrate enhances proliferation and differentiation of osteoblastic MC3T3-E1 cells via AMPK and eNOS activation, Acta Pharmacol. Sin. 32 (2011) 591–600.
[19] B.P. Kota, T.H. Huang, B.D. Roufogalis, An overview on biological mechanisms of PPARs, Pharmacol. Res. 51 (2005) 85–94.
[20] E. Hondares, O. Mora, P. Yubero, M. Rodriguez, R. de la Concepción, R. Iglesias, M. Giralt, F. Villarroya, Thiazolidinediones and rexinoids induce peroxisome proliferator-activated receptor-coactivator (PGC)-1alpha gene transcription: an autoregulatory loop controls PGC-1alpha expression in adipocytes via peroxisome proliferator-activated receptor-gamma coactivation, Endocrinology 147 (2006) 2829–2838.
[21] E. Hondares, I. Pineda-Torra, R. Iglesias, B. Staels, F. Villarroya, M. Giralt, PPARdelta, but not PPARalpha, activates PGC-1alpha gene transcription in muscle, Biochem. Biophys. Res. Commun. 354 (2007) 1021–1027.
[22] E. Hondares, M. Rosell, J. Díaz-Delfín, Y. Olmos, M. Monsalve, R. Iglesias, F. Villarroya, M. Giralt, Peroxisome proliferator-activated receptor α (PPARα) induces PPARγ coactivator 1α (PGC-1α) gene expression and contributes to thermogenic activation of brown fat: involvement of PRDM16, J. Biol. Chem. 286 (2011) 43112–43122.
[23] S. Varum, A.S. Rodrigues, M.B. Moura, O. Momcilovic, C.A. Easley 4th, J. Ramalho-Santos, B. Van Houten, G. Schatten, Energy metabolism in human pluripotent stem cells and their differentiated counterparts, PLoS One 6 (2011) e20914.
[24] W.J. Koopman, H.J. Visch, S. Verkaart, L.W. van den Heuvel, J.A. Smeitink, P.H. Willems, Mitochondrial network complexity and pathological decrease in complex I activity are tightly correlated in isolated human complex I deficiency, Am. J. Physiol. Cell Physiol. 289 (2005) C881–C890.
[25] K. Peng, L. Yang, J. Wang, F. Ye, G. Dan, Y. Zhao, Y. Cai, Z. Cui, L. Ao, J. Liu, Z. Zou, Y. Sai, J. Cao, The interaction of mitochondrial biogenesis and fission/fusion mediated by PGC-1α regulates rotenone-induced dopaminergic neurotoxicity, Mol. Neurobiol. 54 (2017) 3783–3797.
[26] N. Ishihara, M. Nomura, A. Jofuku, H. Kato, S.O. Suzuki, K. Masuda, H. Otera, Y. Nakanishi, I. Nonaka, Y. Goto, N. Taguchi, H. Morinaga, M. Maeda, R. Takayanagi, S. Yokota, K. Mihara, Mitochondrial fission factor Drp1 is essential for embryonic development and synapse formation in mice, Nat. Cell Biol. 11 (2009) 958–966.
[27] J.C. Komen, D.R. Thorburn, Turn up the power – pharmacological activation of mitochondrial biogenesis in mouse models, Br. J. Pharmacol. 171 (2014) 1818–1836.
[28] M. Furuya, J. Kikuta, S. Fujimori, S. Seno, H. Maeda, M. Shirazaki, M. Uenaka, H. Mizuno, Y. Iwamoto, A. Morimoto, K. Hashimoto, T. Ito, Y. Isogai, M. Kashii, T. Kaito, S. Ohba, U.I. Chung, A.C. Lichtler, K. Kikuchi, H. Matsuda, H. Yoshikawa, M. Ishii, Direct cell-cell contact between mature osteoblasts and osteoclasts dynamically controls their functions in vivo, Nat. Commun. 9 (2018) 300.
[29] K.A. Ishii, T. Fumoto, K. Iwai, S. Takeshita, M. Ito, N. Shimohata, H. Aburatani, S. Taketani, C.J. Lelliott, A. Vidal-Puig, K. Ikeda, Coordination of PGC-1beta and iron uptake in mitochondrial biogenesis and osteoclast activation, Nat. Med. 15 (2009) 259–266.
[30] Y. Zhang, N. Rohatgi, D.J. Veis, J. Schilling, S.L. Teitelbaum, W. Zou, PGC1β organizes the osteoclast cytoskeleton by mitochondrial biogenesis and activation, J. Bone Miner. Res. 33 (2018) 1114–1125.